Wave-echo position control of flexible systems: towards an explanation and theory

William J O'Connor

Abstract— **An elegant, novel solution has been developed to the general problem of point-to-point control by a single actuator of a remote load through an intermediate flexible system. It is based on mechanical wave concepts. Under wide-ranging conditions it allows almost "perfect", vibrationless motion of the load. It requires minimal knowledge of the system dynamics and is robust to changes in load, to non-ideal actuator behaviour and to sensing errors. Transit times are excellent. In the start-up the system itself reveals to the controller how to terminate the motion, so that the *real* system acts as the controller *model*. In developing the strategy practice has preceded theory. This paper presents and explores theoretical explanations of the success of the method.**

I. Introduction

From space structures to disk drive heads, from medical mechanisms to long-arm manipulators, from cranes to robots, there are many contexts in which it is desired to achieve rapid and accurate position control of a load (or system end-point) by an actuator that is separated from the load by an intermediate flexible system. While all systems are to some extent flexible, issues related to flexibility become decisive as one tries to design lighter mechanisms, or systems that are more dynamically responsive, or softer, or more energy efficient, or simply long in one dimension.

The system's actuator must then attempt to reconcile two, potentially conflicting, demands: position control and active vibration damping. Somehow each must be achieved while respecting the other's requirements. Previous approaches have included various classical and state feedback control techniques (often using simplified dynamic models); modal control (often considering a rigid-body, or zero frequency mode separately from vibration modes); sliding mode control; input command shaping; bang-bang control; wave-based control; and control based on real-virtual system models. Each method has special characteristics and drawbacks, discussed in the literature [1-19]. None is completely satisfactory under all headings.

Manuscript received 17 September 2003. This work was funded in part by Enterprise Ireland Basic Research Grant, code SC/2001/319/.

W.J. O'Connor is with the Dept of Mechanical Engineering, University College Dublin, National University of Ireland, 213 Engineering Building, Belfield, Dublin 4, Ireland. E-mail: william.oconnor@ucd.ie

Figure 1 shows a simple example of the system type. The position, x_0, of a single actuator, is under computer control. The aim is to manoeuvre the end mass (or "load", at x_n) from rest in one position to rest in a new, target position. The problem is to determine the best strategy in setting $x_0(t)$ to achieve position control of $x_n(t)$.

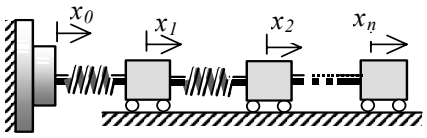

Fig.1 The representative flexible system, with x_0 attempting to control x_n.

The wave-based control strategy developed for this system applies to a very broad class of problems. The number of masses and springs is arbitrary; the load mass can vary in an unknown way between manoeuvres (as can happen for example in robotics); the system can have distributed components, or mixed lumped and distributed; it can have arbitrary internal damping (modeled e.g. as dashpots interconnecting any or all masses); the masses and springs can have arbitrary values, differing throughout the system; and spring and damping characteristics do not even have to be linear (e.g. the springs can "harden" or "soften" with extension). One strategy serves all cases, and does so remarkably well.

II. Background Ideas

In a rigid system, the action and reaction between the load and the actuator are direct and immediate resulting in instantaneous and "perfect" control of the load. In a flexible system, by contrast, the actuator-load interaction is mediated by the flexible dynamics. The load and flexible system dynamics must somehow express themselves at the actuator. The perspective here is that these dynamics reveal themselves at the actuator over time, in response to the actuator's motion, and that when properly detected and responded to, they provide the key to the actuator's recovering control of the remote load. Instantaneous disconnectedness and separation in space, that impede control, can be replaced by mediated interconnection over time, to recover control while respecting the flexible dynamics

From an energy perspective, any initial movement of the actuator injects vibrating kinetic and potential energy into

the system, which then propagates and disperses through the system, partly returning to the actuator. To bring the system to rest again at a target position, all this energy must be absorbed out of the system, completely and exactly, at the instant the system is at target.

As a device to motivate what follows, Fig. 2 shows the original system with a second, mirror-image system appended. The load (or end) masses of the two systems are imagined joined to form a single mass which is therefore double the original load, with a common displacement. The rest of the second system (with primed displacement variables) is identical to the first, but in reverse order, ending in an image actuator. The motion of this image actuator, indicated by x_0, is assumed to follow that of the first actuator exactly.

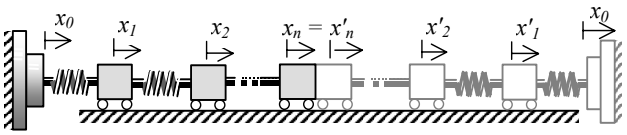

Fig.2 Original system (left) with mirror-image system appended (right). If the displacement of the mirror-actuator (right) follows the original actuator x_0 then the primed displacements will equal the unprimed.

Now if the (assumed equal) motions of the two actuators in Fig.2 are made identical to that of the actuator in the original system, it is readily shown that the response of the left hand side of the combined system in Fig.2 will be identical to that of the original in Fig.1.

Taking a further step, it is postulated that the system in Fig.2 can in turn be considered as the superposition of two such double systems, each a mirror (or reversed-order) image of the other, as depicted in Fig.3. The supposition in Fig.3 is that the motion of each component in the original system will be given by the sum of the corresponding motions in the two systems in Fig.3, and in particular

$$x_0(t) = a_0(t) + b_0(t) \tag{1}$$

$$x_1(t) = a_1(t) + b_1(t) \tag{2}$$

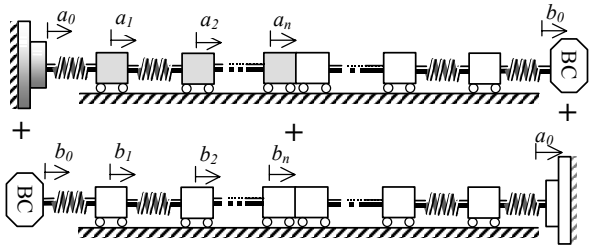

Fig.3 Two perfectly symmetric systems assumed superposed to produce the displacements in Fig.2. Thus $a_i+b_i=x_i$, i = 0, n. "Waves" move from actuator to BC in both cases: i.e., in the second system, from right to left, the arrows indicating reference directions for displacement.

Now the upper system of the pair in Fig.3 can be considered as initiating motion at the left hand end, and, with suitable boundary conditions BC, absorbing it at the right hand end. It takes time for motion initiating at the actuator to move through the system from left to right. "Disturbances" of some kind, or "waves" with associated displacement, velocity, energy and momentum, can be considered as entering the system from the left and (eventually, under certain conditions) leaving to the right. The opposite happens in the lower system.

Now when the "break-out" process has been reversed, the motions of the imaginary actuators and boundaries in Fig.3 become incorporated into the real actuator's motion. The real actuator in the real system can therefore be imagined to be doing at least two jobs in the imagined component systems: initializing motion (or "wave launching") and terminating it ("wave absorbing"). The component motions corresponding to these two jobs will be designated a_0 and b_0, respectively, whose sum will be x_0, the (single) motion of the actuator. See Eq.1. (In what follows, where the meaning is obvious, a and b will mean $a_0(t)$ and $b_0(t)$.)

Inspection of Fig.3 suggests that, for x_n to track x_0, the boundary conditions should be such as to dampen out vibration as quickly as possible while reaching an identical steady state position to that of the actuator: that is active vibration damping and position control. There are many ways to achieve these goals. Perhaps close to optimal is to have the boundary BC simulate an extension of the system with an infinite string of lumped masses and springs matching the system dynamics at the boundary. In this way the energy reflection and dispersion at the boundary are close to minimal. Rapid energy extraction is thereby achieved and the steady state displacement of the boundary BC will be that of the actuator.

If the steady state gain is indeed unity, then, for rest-to-rest motion, the final values of a and b will be equal to each other, and therefore each will equal half the total displacement. In other words if, at the end of the motion, $a_0(t)$ is half the target distance and constant, $b_0(t)$ must also settle at this value.

Furthermore, how $a_0(t)$ reaches this steady value is arbitrary. The idea below is to make the final approach of $a_0(t)$ to the half-target value equal to a time-reversal of the absorbed wave, $b_0(t)$, observed from start-up. Thus, the vibratory echo or signature of the sudden start-up, that worked its way out of the system at BC, is now played back, inverted and time-reversed, at a_0, to produce a time-reversal of the start-up, which, if perfectly achieved, will stop the load dead, and at target.

But first a practical method is needed to separate the actuator's motion into the two components of Eq.1, conveyed in Fig.3.

III. Determining Actuator's Motion, $a(t) + b(t)$

The components $a_0(t)$ and $b_0(t)$ in Fig.3 have no separate physical existence. On the other hand, $x_0(t)$ and $x_1(t)$ do

have physical existence, and can be measured, and from them, under some general assumptions, suitable values for *a* and *b* can be determined, or assigned.

The s-domain transfer function for the displacement of two successive masses in a uniform infinite mass-spring string can be shown to be [11]

$$G_\infty(s) = 1 + \tfrac{1}{2}\left(\frac{s}{\omega_n}\right)^2 \mp \tfrac{1}{2}\sqrt{\left(1+\tfrac{1}{2}\left(\frac{s}{\omega_n}\right)^2\right)^2 - 1} \qquad (3)$$

with $\omega_n = \sqrt{(k/m)}$, k and m the stiffness and mass values.

One can associate the negative sign with a one-directional wave moving in the direction of the main energy flow. In the s-domain, Eq.1 and 2 become

$$X_0(s) = A_0(s) + B_0(s) \qquad (4)$$

$$X_1(s) = A_1(s) + B_1(s) \qquad (5)$$

By collapsing Fig.3 back to Fig.1, and assuming that $G_\infty(s)$ with $\omega_n = \sqrt{(k_1/m_1)}$ describes the transfer function between BC and the first mass in the top half of Fig.3 (and vice versa in the lower half), one gets

$$X_1(s) = G_\infty(s)A_0(s) + B_1(s) \qquad (6)$$

$$= G_\infty(s)A_0(s) + G_\infty^{-1}(s)B_0(s) \qquad (7)$$

This gives the required components as

$$A = X_0 \frac{1}{1-G_\infty^2} - X_1 \frac{G_\infty}{1-G_\infty^2} \qquad (8)$$

$$B = X_0 - A \qquad (9)$$

It is however problematic to get the required time-domain values *a(t)* and *b(t)* from these equations as they stand. Practical algorithms can however be obtained by approximating $G_\infty(s)$ with suitable simpler functions while reformulating Eq. 8, as follows

$$A = X_0 - X_1 G_\infty + A G_\infty^2 \qquad (10)$$

with the second equation from Eq.9 as before. The required variable *A* is no longer explicit in Eq.10. But because the transfer function G_∞^2 on the right hand side has zero instantaneous response, the time implementation of this equation works perfectly well when a "one-time-increment-old" version of *A* is used on the right hand side. In this way, Eq.10 can be made effectively explicit.

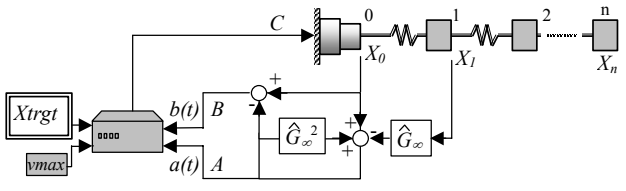

Fig.4. The control system. The box executes the algorithm of Fig.7 with *a(t)* and *b(t)* considered as measured inputs.

Figure 4 has an incorporation of a block diagram implementation of Eqs.9 and 10. The corresponding time implementation is straightforward, with G_∞ and G_∞^2 in Fig.3 replaced by $\hat{G}(s)$ and $\hat{G}^2(s)$, where $\hat{G}$ is modeled by the analogue in Fig.5.

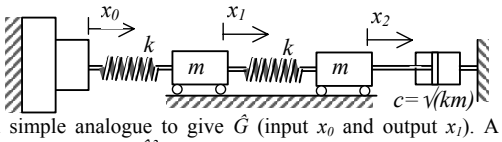

Fig.5. A simple analogue to give $\hat{G}$ (input x_0 and output x_1). A second identical system gives $\hat{G}^2$ but with input x_0 and output x_2. *k* and *m* correspond to the first spring and mass in Fig.1.

Another approach, less computationally demanding, determines, or defines, *a(t)* and *b(t)* simply as follows

$$a(t) = \tfrac{1}{2}\left(x_0(t) + \int \frac{f(t)}{Z}dt\right) = \tfrac{1}{2}\left(x_0(t) + \omega_n \int (x_0 - x_1)dt\right) \qquad (11)$$

$$b(t) = \tfrac{1}{2}\left(x_0(t) - \int \frac{f(t)}{Z}dt\right) = \tfrac{1}{2}\left(x_0(t) - \omega_n \int (x_0 - x_1)dt\right) \qquad (12)$$

where *f(t)* is the force at the actuator, acting in the first spring, and *Z* is an impedance value of $\sqrt{(km)}$. This works surprisingly well, even if further from the conjectured optimal.

IV. The Control System

The challenge set at the outset was "simply" to specify $x_0(t)$ so as to move x_n from rest to rest at a new target position. To repeat, the actuator motion, $x_0(t)$ is considered as the superposition of two component motions, $a_0(t)$ and $b_0(t)$. The first component, $a_0(t)$, is set (by the controller) to a carefully specified value over time. Speaking loosely, this gives the system a controlled push, or launches motion (or a "wave") into the system, the total and final value of which is half the target distance. The controller observes the system response throughout. From this it determines $b_0(t)$, and moves to absorb this "returning wave" by adding $b_0(t)$ to $a_0(t)$, to get the (total), reconstituted actuator position $x_0(t)$ over time.

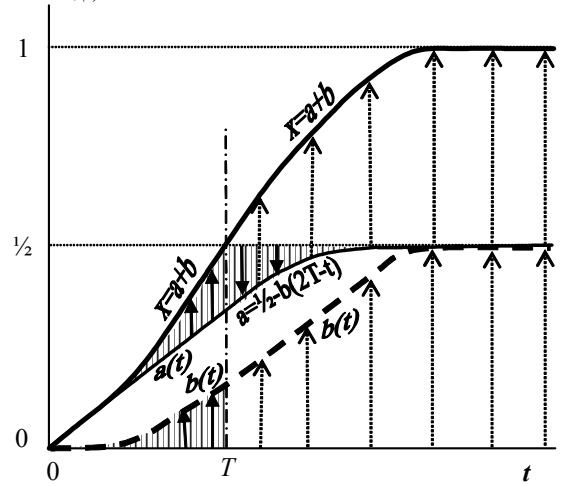

Fig.6. The notional separation and recombination of *x(t)* by way of *a(t)* and *b(t)*. The fine hatching and arrows suggests equal areas, and how they are determined. *a(t)* is ramped until *T*, when it begins to play back the recorded *b(t)* up to that point, but inverted. $x(t) = a(t) + b(t)$ for all *t*.

Figure 6 shows an example, with variables tracked over time. The target distance is unity. In this case, the controller

initially assigns a ramp input to *a* and adds to this the observed *b* to produce the actuator request position *x*. Then, when the sum of *a+b* reaches half the target distance, at time *t=T*, the new assigned value of *a(t)* is *½-b(2T-t),* in other words, the final value minus the time reversed value of *b(t)* up to this point. The controller continues to add to this new *a(t)* the observed value of *b(t)*, which also ends up at ½, ensuring that *x(t)* ends up at 1.0. But it ends up at the target in a way that brings the system to rest very elegantly, as will be seen.

Figure 4 shows a box that executes the algorithm in Fig.7 to achieve this. It takes *a(t)* and *b(t)* as inputs and produces the actuator position request, *c(t)*, as output. Two further inputs are the target displacement, *xtrgt*, and a maximum actuator velocity, *vmax*. The essence of the algorithm to be evaluated at each time step, *t*, is as follows:

```
1    IF a(t)+b(t)< ½xtrgt      Still in 1st launch stage?
     AND stage=1               Without having left it?
2      R(t) = ∫(½ vmax)dt      Assign i/p (launch) position
3      echo(t) = b(t)          Record echo b(t)
4      T = t                   T marks end of 1st stage
5    ELSE IF (2T-t)>0          Not yet run out of echo?
6      r(t) = ½ xtrgt          Set i/p = final value minus
         -echo(2T-t)           time-reversed echo
7      Stage=2                 Avoids re-entering stage 1
8    ELSE                      End of echo?
9      R(t) = xtrgt-a(t)       Set i/p as in Fig.12
10   END
11     C(t) = r(t) + b(t)      For all i/p "cancel" b(t)
```

Fig.7. Algorithm executed by the computer in Fig.5 for rest to rest motion. *a(t)*, *b(t)* are determined for each time step *t*, by any of the methods described. The variable *stage* is initialised to 1 outside the control loop. *xtrgt* and *vmax* are specified elsewhere.

The variable *r(t)* is the assigned input before superposing *b(t)*. For an ideal actuator, *r(t)=a(t)*, and $x_0(t) = c(t)$. Lines 1-10 determine *r(t),* for all stages, and line 11 adds *b(t)*, again for all stages.

V. Sample Results

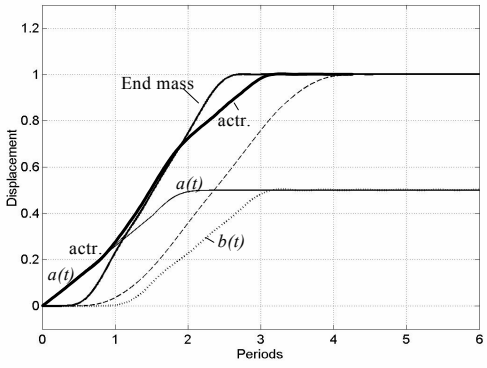

Fig. 8. End point of a uniform, three-mass system, moved 1m.

Figure 8 shows the performance of this algorithm applied to a numerical model of a uniform three-mass system. The actuator and end-mass positions are shown against time expressed in units of the period, T, or $t\omega_n/2\pi$. The target displacement is 1 *m*. Also shown are *a(t)* and *b(t)*.

By any standards, this is a remarkable result. The load (end mass) is translated from rest to rest, in a single, controlled movement, with almost no overshoot and with negligible oscillations (and so little or no settling time). The end mass comes to rest exactly at target, and earlier than the actuator, which is remotely controlling its motion. For much of the time, the speed of the load (slope in Fig.8) is close to that of the actuator, as if the flexible system were stiff. Throughout the motion the actuator's movements are gentle and smooth.

The variable *vmax* acts as a speed control and sets the slope of the response for the main part of the motion. Assuming the actuator speed limit is not an issue, then simply by adjusting *vmax* one can make a classical control trade-off between, on the one hand, the end-mass rise-time, and, on the other, the degree of overshoot and settling time. Figure 9 shows some examples for a three mass system.

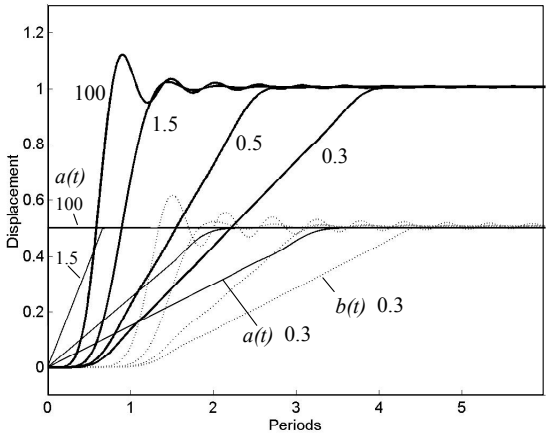

Fig.9. End mass response for values of *vmax* of 100, 1.5, 0.5 & 0.3 times trgt/T. *a(t)* and *b(t)* also shown for the four cases. For largest *vmax*, *a(t)* is effectively a step input.

Setting *vmax* very high shortens the rise-time. But even in the "worst" case with *vmax* effectively unlimited (100**trgt/T* in Fig.9), and therefore *a(t)* taking the form of a step input, the overshoot and the amplitude of the residual oscillations are small, and have died out before the arrival time of the time-optimal case. Going in the other direction, reducing *vmax* increases the manoeuvre time, soon achieving almost zero overshoot and negligible residual vibration. The actuator may have a physical speed limit that is below that of the ideal actuator when achieving an optimum response. In this case, *vmax* in the controller can be set to this speed limit. For the main part of the motion, the load will then be at this maximum actuator speed (the maximum speed if the system were rigid); the absorbing action will still work without hitting the saturation limit (ensured by

the "½" in the initial input of *a(t)*); and there will be even less residual vibration on arrival at target.

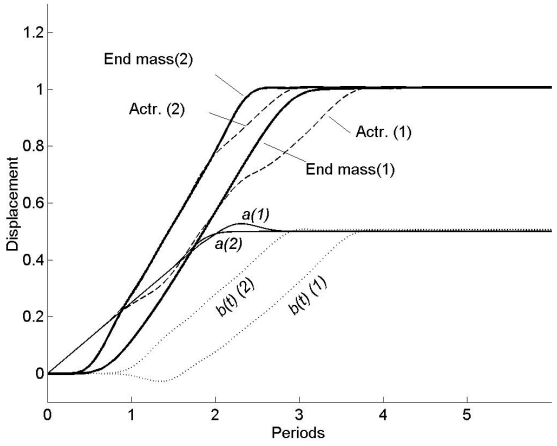

Fig.10. Three masses with end mass multiplied by 3 (case 1) and by 1/3 (case 2) and controller parameters unchanged from those of the uniform case (Fig.8).

Remarkable as all this may seem, the good news does not end there. The new control strategy is found to be surprisingly robust and self-adapting. The strategy has no difficulty coping with significant changes in the system remote from the actuator. Figure 10 for example shows the result with the end/load mass increased by three (case 1) and then reduced to one third (case 2), but without changing a single control parameter from the uniform case of Fig.9.

The strategy also works for any number of degrees of freedom, large or small. Going for the smallest, Fig.11 shows a response for a one mass system. The only adjustment to the controller was to set *vmax* to 1.5**trgt/T* for the case shown. If preferred, the tiny overshoot and settling can be yet further reduced by simply reducing *vmax* a little (cf. Fig.9 for 3 DOF case), at the cost of a slightly longer transit time.

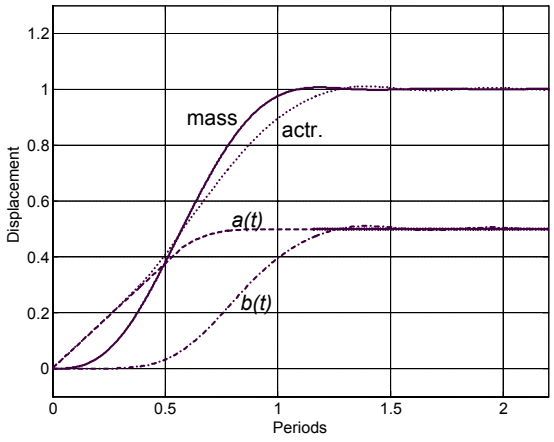

Fig.10. Response of 1 DOF system with *vmax*=1.5*trgt/T.

Other such changes in the internal dynamics of the flexible system, that with other strategies often require a complete rethink, are here handled automatically. For example, add internal damping or make the springs non-linear, and the same strategy still works very well. If part of the system is distributed (continuous) rather than lumped, again there are no new control issues to be grappled with.

For an ideal actuator, $x_0(t) = c(t)$ and $r(t) = a(t)$. But a real actuator will take time to respond, so these equalities will apply only at steady state. A further extraordinary feature of the new algorithm is that it still performs well with a far from ideal actuator. Provided the actuator's steady state position error is zero and its bandwidth is sufficiently high in comparison with the highest natural frequency of the system, performance is still very good. (For a uniform system of any length, the highest natural frequency is $2\omega_n$.)

As a final example, illustrating a mixture of such added complexities, Fig.12 shows the response of a 5 DOF system with non-linear (hardening) springs; variations of the masses of 1, 0.5, 1, 2, 1; damping between the masses of 0, 0.25, 0.1, 0.25, 0, 0.05 times critical damping; an actuator modelled as a first order system of time constant $1/3\omega_n$; and *a(t)* and *b(t)* approximated by Eqs.11 & 12. These values and the system size were chosen almost at random: a similar result is obtained for almost arbitrary choices of these variables.

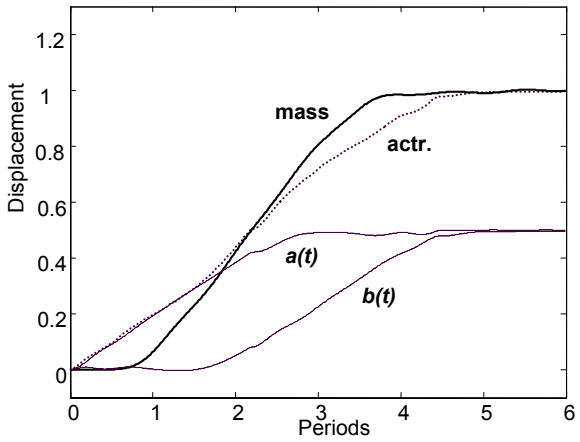

Fig.12. Response of end mass of 5 DOF system, with non uniform masses, various dampers between the masses, non-linear springs, a first order actuator, and an simple approximation for *a(t)* and *b(t)*.

VI. Open-ended, varying input control

The main topic of this paper is controlled motion through a desired distance from rest to rest. But for completeness, it is noted that the strategy outlined above can be adapted for "open-ended" control, where the final position may not be known beforehand, or the input may be arbitrary or unpredictable, or the system may not be at rest initially. Figure 13 shows an arrangement for this, in which input X(s) (or

x(t)) is arbitrary. The response to a step input for this arrangement is almost identical to that of the high *vmax* curve in Fig.9: no longer "vibrationless", but still an excellent response.

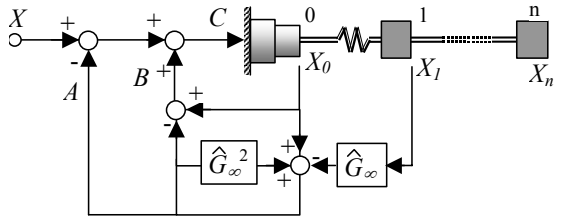

Fig.13 The strategy adapted for open-ended control, with arbitrary input X. Ref.19 describes how this can be still further simplified.

VII. CONCLUDING REMARKS

Many configurations in addition to those shown above have been simulated and comprehensively tested in numerical simulations, in all cases giving similarly impressive responses. The same control strategy has also been demonstrated experimentally on a gantry crane model, again with excellent results.

The algorithm gets the system to reveal its dynamics to the controller so the controller then knows exactly how to stop the load dead at target. Other than a single assumed parameter (e.g. ω_n) the only system "model" the controller uses is the real system itself, partly explaining the strategy's robustness and generic nature. Modelling errors do not feature and system changes are automatically accommodated. For example, the order of the controller automatically matches that of the system, and explicit information, for example, about locations of poles (or natural frequencies and damping ratios of modes) is not needed. The real system is also the controller's main "computer", as it "calculates" the exact echo profile, which the controller simply observes and records for use in stage 2.

For various reasons it is difficult to compare these results directly with acceleration-limited time-optimal control [12]. Suffice it to say here that the wave-based results for the cases presented are hardly affected if one limits the actuator acceleration to a reasonable value. Indeed, if one defines settling time in a standard textbook way, wave-based control could claim in some cases to be faster than time-optimal! In any case, wave-based control involves considerably less energy and has no need for accurate switching times, nor high jerk, nor an accurate system model, nor the difficult switching time calculations, nor the ideal actuator, all of which are required by the time optimal control approach.

All aspects of the new strategy merit further analysis and investigation. This work is under way. Work has also begun on applying the same ideas to more complex systems, including systems with multiple actuators, whether in series or in parallel, and systems undergoing flexural vibrations. Initial results are very promising.

Although involving some subtleties and unconventional approaches, the new strategy is essentially simple and intuitive. It is hard to believe it has not been discovered long ago.

REFERENCES

[1] Meirovitch, L., 1989, Dynamics and Control of Structures, Wiley.

[2] Preumont, A., 1997, "Vibration control of active structures", Kluwer Academic Publishers, Netherlands.

[3] Book, W. J., 1993, "Controlled Motion in an Elastic World," ASME Journal of Dynamic Systems, Measurement, and Control, 115, June 1993, pp. 252-261.

[4] Vincent, T. L., Joshi, S. P., 1989, Yeong Ching Lin, "Positioning and Active Damping of Spring-Mass Systems," ASME Journal of Dynamic Systems, Measurement, and Control, 111, Dec. 1989, pp. 592-599.

[5] Jayasuriya, S., Choura, S., 1991, "On the Finite Settling Time and Residual Vibration Control of Flexible Structures," Journal of Sound and Vibration, 148, No.1, 1991, pp. 117-136.

[6] Book, W.J., 1984, "Recursive Lagrangian Dynamics of Flexible Manipulator Arms", International Journal of Robotics Research 3, (3), 1984, pp.87-101.

[7] Yamada, I., Nakagawa, M., 1985, "Reduction of Residual Vibration in Position Control Mechanisms," ASME Journal of Vibration, Acoustics, Stress, and Reliability in Design, 107, Jan. 1985, pp. 47-52.

[8] Feliu, J.J., Feliu, V., Cerrada C., 1999, "Load adaptive control of single-link flexible arms based on a new modelling technique", IEEE Trans Robotics and Automation, 15, no.5, pp.793-804, Oct 1999.

[9] Singh, T., Heppler, G. R., 1993 "Shaped Input Control of a System with Multiple Modes", ASME Journal of Dynamic Systems, Measurement and Control, 115, September 1993, 341-347.

[10] Singhose, W. E., Singer, N. C., Seering, W. P., 1994 "Design and Implementation of Time-Optimal Negative Input Shapes," Proceedings of the 1994 International Mechanical Engineering Congress and Exposition, Chicago, IL, USA. ASME Dynamic Systems and Control Division (publication) DSC 55-1, 1994, pp. 151-157.

[11] O'Connor, W.J., Lang D., 1998: "Position Control of Flexible Robot Arms using Mechanical Waves", ASME Journal of Dynamics Systems, Measurement and Control, 120, no.3, pp.334-339, Sept 1998.

[12] Pao, L.Y. 1996: "Minimum-time Control Characteristics of Flexible Structures", AIAA Journal of Guidance, Control and Dynamics, 1, pp.123-129, Jan-Feb 1996.

[13] Abduljabbar, Z., ElMadany, M. M., Al-Dokhiel, H. D., 1993, "Controller Design of a One-link Flexible Robot Arm," Computers and Structures, 49, No. 1, 1993, pp. 117-126.

[14] O'Connor, W.J., 2002, "Gantry crane control: a novel solution explored and extended", Proceedings ACC02, Alaska, 8 May 2002.

[15] O'Connor, W.J. 2003: "A gantry crane problem solved", ASME J. Dyn. Sys., Meas., Control 125, 4, 569-576, Dec. 2003 Dec. 2003

[16] Karolov, V. V., Chen, Y. H., 1989, "Controller Design Robust to Frequency Variation in a One-link Flexible Robot Arm," ASME Journal of Dynamic Systems, Measurement, and Control, 111, March 1989, pp. 9-14.

[17] Meckl, P., Seering, W., Active vibration damping in a three-axis robotic manipulator, ASME Journal of Vibration, Acoustics, Stress and Reliability in Design, 107, Jan 1985, pp.38-46.

[18] Muenchhof, M., Singh, T., 2003, "Jerk limited time optimal control of flexible structures", ASME Journal of Dynamic Systems, Measurement, and Control, 125, 1, March 2003, pp. 139-142.

[19] O'Connor, W.J., Hu, Chunmin, 2002, "A simple, effective position control strategy for flexible systems", International Federation of Automatic Control, 2nd IFAC Conference on Mechatronic Systems, Dec, 2002, Berkeley, California, USA, pp 153-158.